代表文章 4

本论文研究了以 2-溴酚、2,4-二溴苯酚和 2,4,6-三溴苯酚为前体物形成多溴代二噁英(PBDD/Fs)的气相形成机制。整个过程采用密度泛函理论(DFT)进行计算。首先在 MPWBlK/6-31+G(d,p) 水平下计算了各驻点的几何构型和振动频率，相应的能量参数在 MPWBlK/6-311+G(3df,2p) 水平下完成。然后将多溴代二噁英(PBDD/Fs)的形成机理与 2-氯酚、2,4-二氯苯酚和 2,4,6-三氯苯酚为前体物形成多氯代二噁英(PCDD/Fs)相比。最后，使用小曲率隧道(SCT)校正的正则变分过渡态理论(CVT)计算了 600-1200 K 温度范围内的重要基元反应的速率常数。研究表明，只有邻位有溴取代基的溴酚才能形成 PBDDs。结合我们以前的研究，可以明显地看出由溴酚形成 PBDDs 比由氯酚形成 PCDDs 更容易。溴取代数目的增多抑制了 PBDD/Fs 的形成。

Mechanism and Direct Kinetics Study on the Homogeneous Gas-Phase Formation of PBDD/Fs from 2-BP, 2,4-DBP, and 2,4,6-TBP as Precursors

Wanni Yu, Jingtian Hu, Fei Xu, Xiaoyan Sun, Rui Gao, Qingzhu Zhang,* and Wenxing Wang

Environment Research Institute, Shandong University, Jinan 250100, P. R. China

S *Supporting Information*

ABSTRACT: This study investigated the homogeneous gas-phase formation of polybrominated dibenzo-*p*-dioxin/dibenzofurans (PBDD/Fs) from 2-BP, 2,4-DBP, and 2,4,6-TBP as precursors. First, density functional theory (DFT) calculations were carried out for the formation mechanism. The geometries and frequencies of the stationary points were calculated at the MPWB-1K/6-31+G(d,p) level, and the energetic parameters were further refined by the MPWB1K/6-311+G(3df,2p) method. Then, the formation mechanism of PBDD/Fs was compared and contrasted with the PCDD/F formation mechanism from 2-CP, 2,4-DCP, and 2,4,6-TCP as precursors. Fi-

nally, the rate constants of the crucial elementary reactions were evaluated by the canonical variational transition-state (CVT) theory with the small curvature tunneling (SCT) correction over a wide temperature range of 600−1200 K. Present results indicate that only BPs with bromine at the ortho position are capable of forming PBDDs. The study, together with works already published from our group, clearly shows an increased propensity for the dioxin formations from BPs over the analogous CPs. Multibromine substitutions suppress the PBDD/F formations.
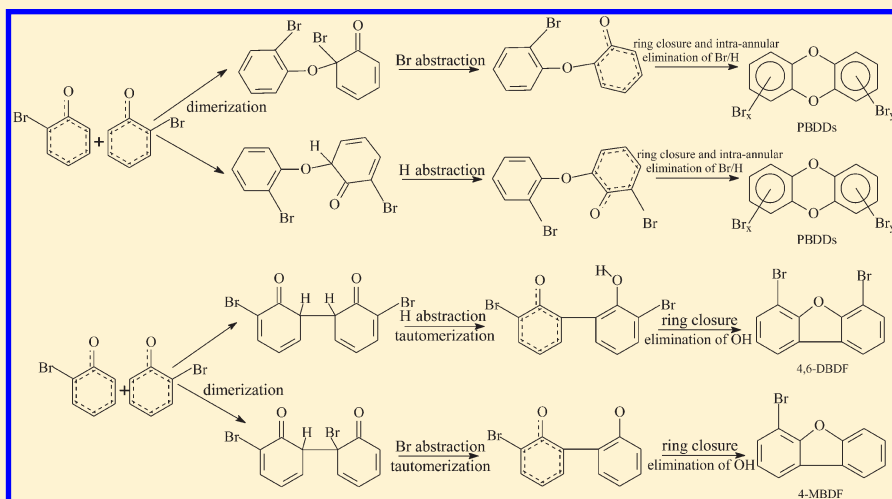
■ INTRODUCTION

Polybrominated dibenzo-*p*-dioxin/dibenzofurans (PBDD/Fs) are polychlorinated dibenzo-*p*-dioxin/dibenzofurans (PCDD/Fs) analogues in which all of the chlorine atoms are substituted by bromine atoms. Therefore, they have similar physicochemical properties, toxicity, and geochemical behavior in the environment.[1−6] PBDD/Fs are known to occur unnaturally and to be produced unintentionally as unwanted byproduct. Recently, the level of environmental concern regarding PBDD/Fs has been raised[7−9] because of the rapid increase in the use of brominated flame retardants (BFRs). PBDD/Fs can be formed in the process of manufacturing BFRs. In particular, a large quantity of PBDD/Fs is emitted from electronic waste recycling and the pyrolysis or combustion of waste materials containing BFRs.[10−15]

The high correlation between the PBDD/F and PCDD/F concentrations revealed their similar formation mechanism in the pyrolysis or combustion system.[12,13] Chlorophenols (CPs) are key intermediates in essentially all proposed pathways of the formation of PCDD/Fs.[16,17] Similarly, bromophenols (BPs) have been demonstrated to be the precursors of

PBDD/Fs.[8,18−20] BPs are extensively used as flame retardants, intermediates for the yield of other flame retardants, and pesticides for wood preservation. In addition, BPs may be released into the environment as major degradation products of other BFRs.[21] Under pyrolysis or combustion conditions, PBDD/F can be formed from BPs by two general reactions: homogeneous gas-phase reactions and heterogeneous metal-mediated reactions. It is generally believed that gas-phase mechanism accounts for about 30% of the total PBDD/F emissions, and surface-mediated mechanism is responsible for the remainder.[18]

Compared to the situation for PCDD/Fs, there are very few studies on the formation of PBDD/Fs. This is largely due to shortage of commercial available PBDD/Fs' standards for quantification.[6,11,22,23] Here, therefore, we conducted a direct density functional theory (DFT) kinetics study on the
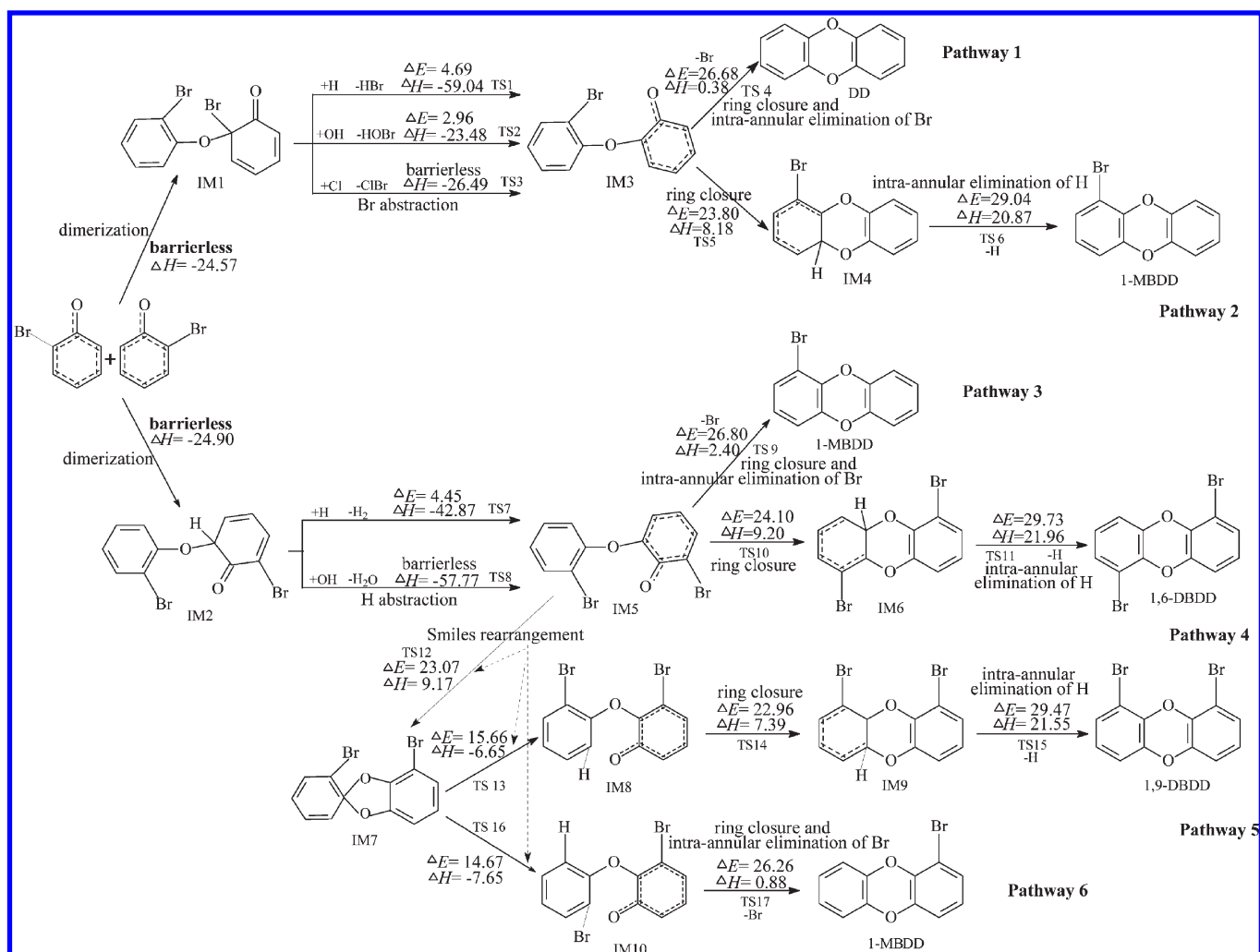
Figure 1. PBDD formation routes embedded with the potential barriers ΔE (in kcal/mol) and reaction heats ΔH (in kcal/mol) from 2-BP as precursor. ΔH is calculated at 0 K.

homogeneous gas-phase formation of PBDD/Fs from 2-BP, 2,4-DBP, and 2,4,6-TBP as precursors, which are the most widely manufactured BPs and the most abundant BPs found in waste incinerators. The primary objective of the study is to elucidate the homogeneous gas-phase formation mechanism of PBDD/Fs from BPs. A second objective is to deduce the rate constants of the key elementary reactions involved in the PBDD/F formations. Further interest is planed to focus on the homogeneous gas-phase formation of 2,3,7,8-TeBDD, which is the most toxic among all 210 PBDD/F isomers, as well as the heterogeneous metal-mediated formation of PBDD/Fs.

■ COMPUTATIONAL METHODS

The density functional theory (DFT) calculations were performed using the Gaussian 03 package.[24] All geometries were fully optimized at the MPWB1K/6-31+G(d,p) level.[25] The nature of various stationary points was determined by frequency calculations. To check whether the obtained transition states connect the right minima, the intrinsic reaction coordinate (IRC) calculations were carried out. To improve the reaction heat and potential barrier, the single point energies

were calculated at the MPWB1K/6-311+G(3df,2p) level. By means of the Polyrate 9.3 program,[26] the rate constants were computed by the canonical variational transition-state (CVT) theory[27−29] with the small curvature tunneling (SCT) contribution.[30]

■ RESULTS AND DISCUSSION

The optimized geometries of 2-BP and DD at the MPWB1K/6-31+G(d,p) level are in reasonable accordance with the corresponding experimental values, and the largest discrepancy remains within 1.5% for the bond lengths.[31,32] For the reaction of 2-BP+2-BP→DD+H$_2$+Br$_2$, the reaction enthalpy of 29.22 kcal/mol calculated at the MPWB1K/6-311+G(3df,2p) level and at 298.15 K agrees well with the experimental value of 30.52 kcal/mol, which is derived from the experimental standard enthalpies of formation.[33−35]

Formation of 2-BPRs, 2,4-DBPRs, and 2,4,6-TBPRs. It has shown that the homogeneous gas-phase formation of PBDD/Fs is attributed to the dimerization of bromophenoxy radicals (BPRs).[36,37] Thus, the formation of BPRs is the initial step in the formation of PBDD/Fs. Under pyrolysis or combustion conditions, BPRs can be readily formed from BPs through
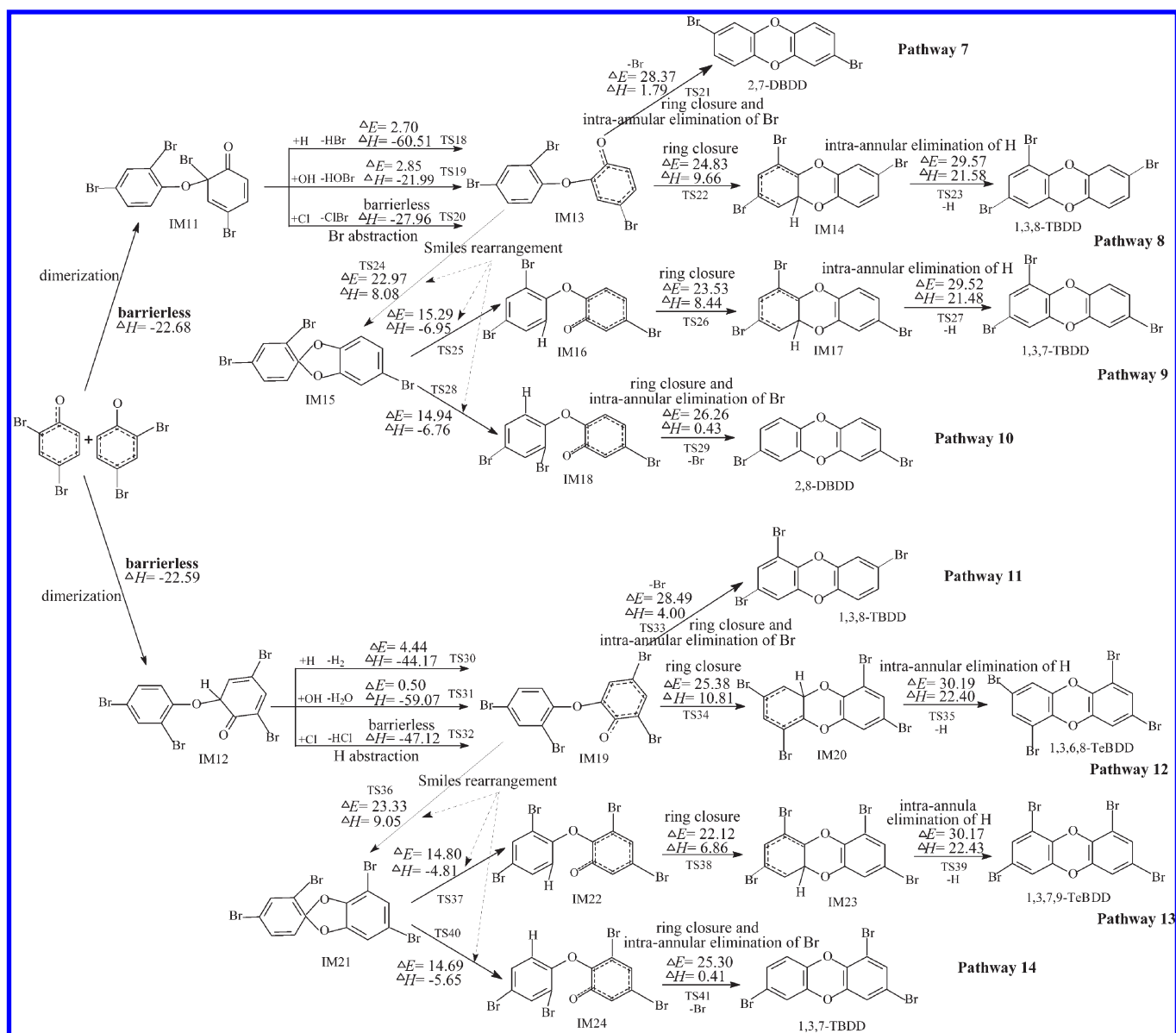
1918

dx.doi.org/10.1021/es103536t |*Environ. Sci. Technol.* 2011, 45, 1917–1925

Figure 2. PBDD formation routes embedded with the potential barriers ΔE (in kcal/mol) and reaction heats ΔH (in kcal/mol) from 2,4-DBP as precursor. ΔH is calculated at 0 K.

loss of the phenoxyl-hydrogen by unimolecular, bimolecular, or possibly other low-energy pathways (including heterogeneous reactions).[36,37] The unimolecular reaction occurs via the decomposition of BPs with the cleavage of the O–H bond. The bimolecular reactions proceed through the phenoxyl-hydrogen abstraction from BPs by the active radicals, H, OH, O (^{3}P), Cl, and Br, which are abundant in the combustion environment.[36,37] The potential barriers (ΔE) and reaction heats (ΔH, 0 K) calculated at the MPWB1K /6-311+G(3df,2p) level are presented in the Supporting Information.

Formation of PBDDs. *Formation of PBDDs from the Dimerization of 2-BPRs.* Six possible PBDD formation pathways, illustrated in Figure 1, are proposed from 2-BP. As seen from Figure 1, all PBDD formation pathways start with oxygen–carbon coupling, followed by Br or H abstraction. The oxygen–carbon coupling is a barrierless and strongly exothermic process.

All of the Br or H abstraction steps are highly exothermic with low-energy barriers. In pathways 1, 3, and 6, ring closure and intra-annular elimination of Br occur in a one-step reaction and are the rate determining step. There is a Smiles rearrangement after H abstraction in pathways 5 and 6, respectively. Intra-annular elimination of H is the rate determining step for pathways 2, 4, and 5 due to the high barrier and strong endothermicity.

Obviously, pathway 1 covers relatively less elementary steps compared to pathway 2. Furthermore, the rate determining step involved in pathway 1 has a lower barrier and is much less endoergic than that involved in pathway 2. Thus, pathway 1 is favored over pathway 2. Similarly, pathway 3 is favored over pathway 4. Pathway 6 is favored over pathway 5. Therefore, the thermodynamically favorable PBDD formation pathways are pathways 1, 3, and 6, leading to the formation of DD and 1-MBDD, consistent with the experimental observation.[36,37]
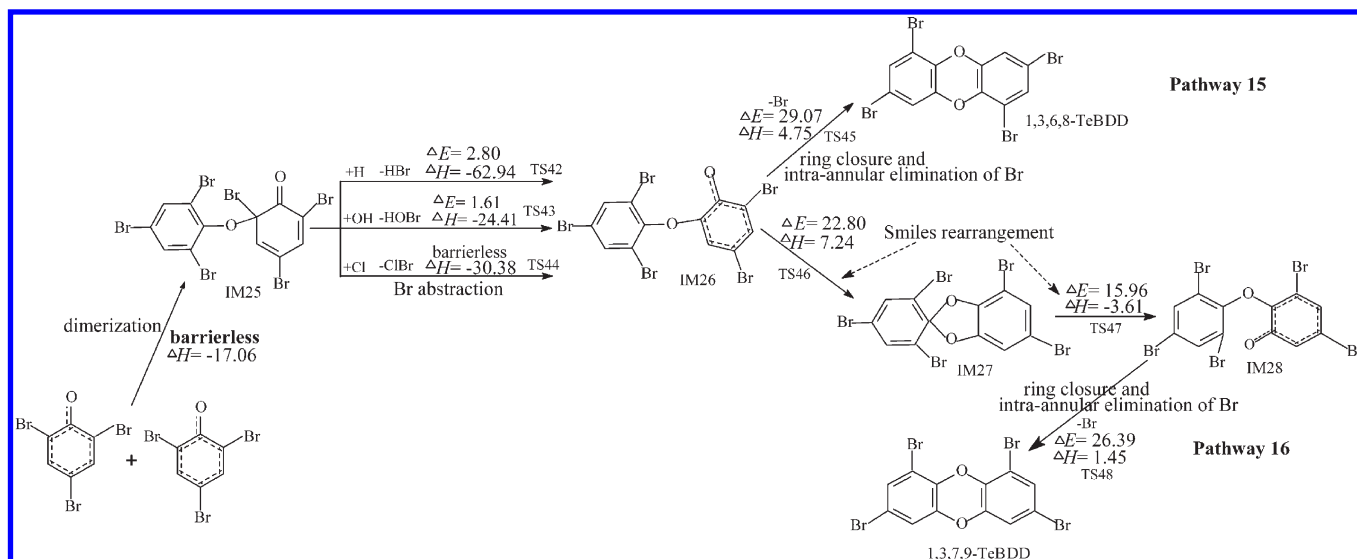
Figure 3. PBDD formation routes embedded with the potential barriers ΔE (in kcal/mol) and reaction heats ΔH (in kcal/mol) from 2,4,6-TBP as precursor. ΔH is calculated at 0 K.

Comparison of the PBDD formations from 2-BP with the previous study for 2-CP[38] clearly shows that intra-annular elimination of Br is much less endothermic than the analogous intra-annular elimination of Cl because of the weaker C—Br bond versus C—Cl bond, resulting in the formation of DD being more favorable from 2-BP than 2-CP. The result is supported by the experimental evidence that the maximum yield for the DD formation from 2-BP is 20 times higher than that from 2-CP.[36,37]

Formation of PBDDs from the Dimerization of 2,4-DBPRs and 2,4,6-TBPRs. Eight possible reaction pathways are postulated to explain the formation of PBDDs from 2,4-DBP. The formation schemes embedded with the potential barriers and reaction heats are depicted in Figure 2. Similar to the mechanism suggested for 2-BP, all PBDD formation pathways start with oxygen—carbon coupling, followed by Br or H abstraction. In pathways 7, 10, 11, and 14, ring closure and intra-annular elimination of Br occur in a one-step reaction and are the rate determining step. Intra-annular elimination of H is the rate determining step for pathways 8, 9, 12, and 13. It is clear from Figure 2 that PBDDs are preferentially formed from pathways 7, 10, 11, and 14. The resulting 2,7-DBDD, 2,8-DBDD, 1,3,7-TBDD, and 1,3,8-TBDD are the dominant PBDD products.

Due to the symmetry of 2,4,6-TBP, only two PBDD formation pathways, pathways 15 and 16, were identified and displayed in Figure 3. Pathway 16 contains two more elementary steps than pathway 15. Nevertheless, the rate determining step involved in pathway 15 requires a higher barrier and is more endothermic than that involved in pathway 16. So, pathways 15 and 16 should be competitive. The resulting 1,3,6,8-TeBDD and 1,3,7,9-TeBDD were experimentally detected in the pyrolysis of 2,4,6-TBP.[23,39] Comparison with the previous work[40] suggests that the formation of PBDDs from 2,4,6-TBP is relatively easier compared to the formation of the analogous PCDDs from 2,4,6-TCP because Br is a better leaving group than Cl.

Mechanisms presented in Figure 1, Figure 2, and Figure 3 show that the rate determining step to the PBDD formations is intra-annular elimination of Br or H. Intra-annular elimination of H has a higher barrier and is much more endothermic than intra-annular elimination of Br. The thermodynamically favorable PBDD formation pathways occur through intra-annular elimination of Br. The Br atom, which is eliminated, is the substituent at the ortho position in BPs. This implies that only BPs with bromine at the ortho position are capable of forming PBDDs. The result is similar to that observed for the PCDD formations from CPs.[41] Comparison of the PBDD formations from 2-BP, 2,4-DBP, and 2,4,6-TBP clearly indicates that the formation mechanism is controlled largely by the substitution pattern of BPs. The exothermicity of the oxygen—carbon coupling decreases with increasing number of bromine substitutions. Although one ortho-bromine is needed for the formation of PBDDs, multi-bromine substitutions suppress the dimerization of BPRs, i.e., suppress the formation of PBDDs.

Formation of PBDFs. 4,6-DBDF and 4-MBDF were experimentally observed in the high-temperature oxidation of 2-BP.[37] Two reaction routes, presented in Figure 4, are offered to interpret the formation of 4,6-DBDF. Pathway 17 involves five elementary processes: carbon—carbon coupling, H abstraction, tautomerization (H-shift), ring closure, and elimination of OH. The ring closure process has a large barrier and is strongly endoergic, and it is the rate determining step. Pathway 18 also involves five elementary processes: carbon—carbon coupling, tautomerization (double H-transfer), H abstraction, ring closure (the rate determining step), and elimination of OH. Pathway 19 in Figure 4 illustrates 4-MBDF being formed from 2-BP. The o,o'-dihydroxybiphenyl intermediate IM29 can be regarded as a prestructure of 4,6-DBDF, and IM34 is a prestructure of 4-MBDF. It can be seen from Figure 4 that the formation of IM29 is more exothermic than the formation of IM34. Moreover, the rate determining step involved in the formation of 4,6-DBDF has a lower barrier and is less endothermic than that involved in the formation of 4-MBDF. Thus, the formation of 4,6-DBDF is preferred over the formation of 4-MBDF.

Similar to the formation of PBDFs from 2-BP, two PBDF congeners, 2,4,6,8-TeBDF and 2,4,8-TBDF, can be formed
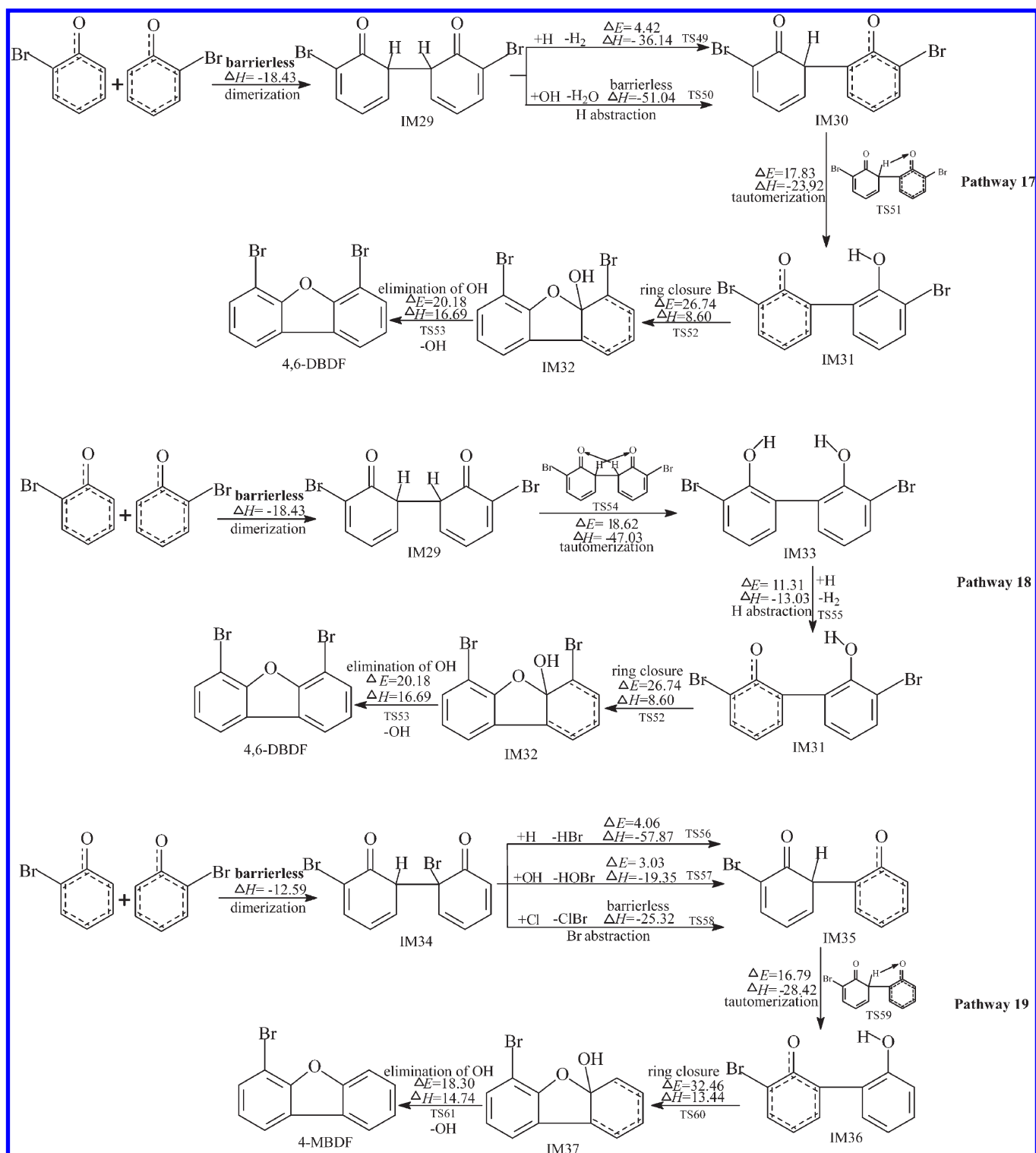
Figure 4. PBDF formation routes embedded with the potential barriers ΔE (in kcal/mol) and reaction heats ΔH (in kcal/mol) from 2-BP as precursor. ΔH is calculated at 0 K.

from 2,4-DBP. The formation mechanism is schemed in Figure 5. Evidently, the formation of 2,4,6,8-TeBDF is preferred over the formation of 2,4,8-TBDF. Comparison of the reaction pathways presented in Figure 4 and Figure 5 shows that the substitution pattern of BPs has a significant effect on the formation mechanism of PBDFs. The

arbon−carbon coupling of 2-BPRs is more exothermic compared to the carbon−carbon coupling of 2,4-DBPRs. Because both ortho-positions are substituted with the voluminous bromine atoms, the carbon−carbon coupling of 2,4,6-TCPRs is sterically inhibited. So, no PBDFs can be formed from 2,4,6-TBP.
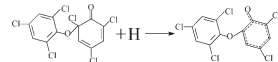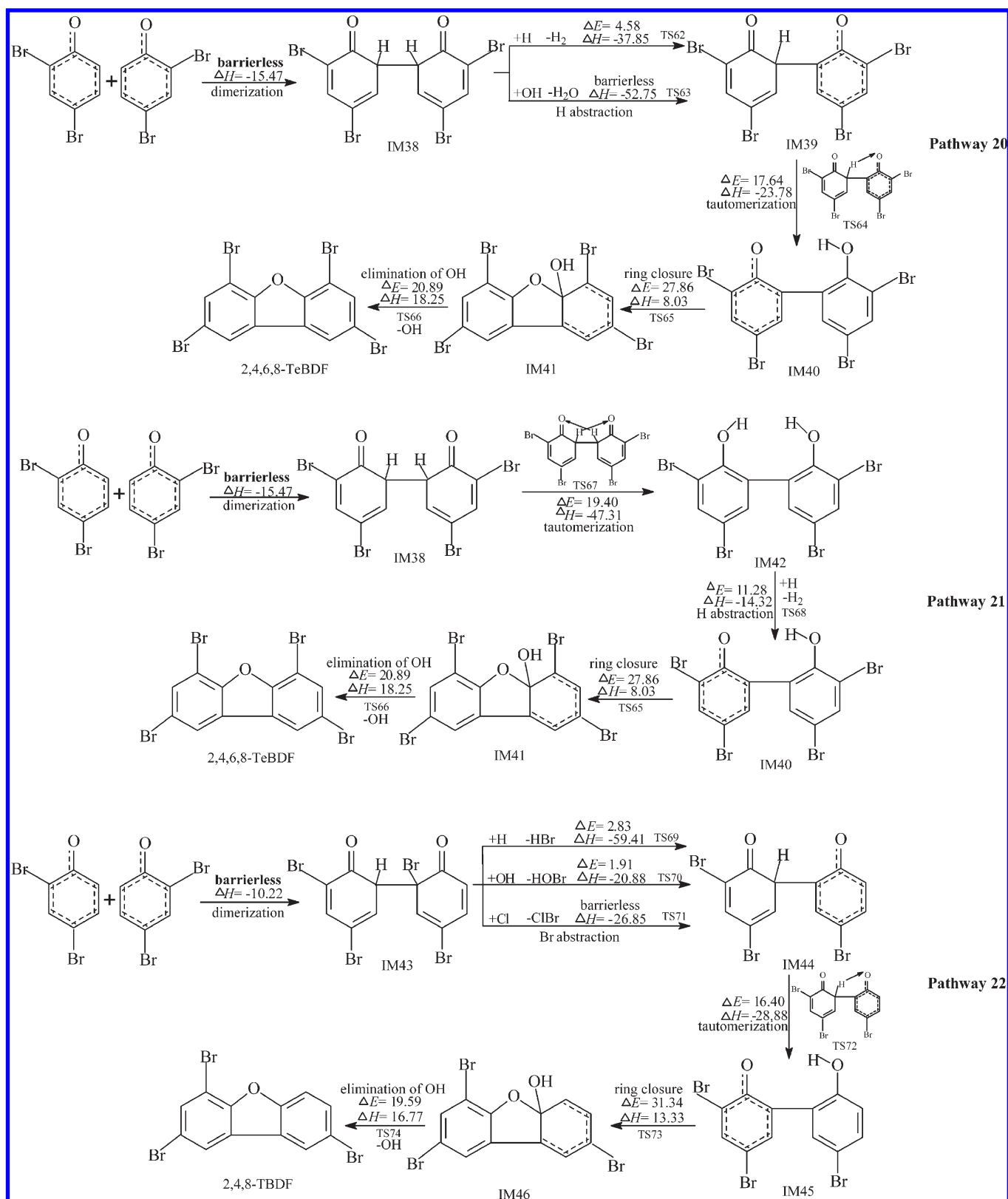
1921

dx.doi.org/10.1021/es103536t |*Environ. Sci. Technol.* 2011, 45, 1917–1925

Figure 5. PBDF formation routes embedded with the potential barriers ΔE (in kcal/mol) and reaction heats ΔH (in kcal/mol) from 2,4-DBP as precursor. ΔH is calculated at 0 K.

Rate Constant Calculations. Previous researches have shown that the CVT/SCT rate constants of $C_6H_5OH+H\rightarrow C_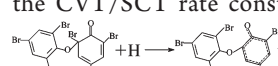6H_5O+H_2$, $C_6H_5OH+OH\rightarrow C_6H_5O+H_2O$ match well with the corresponding experimental values.[42,43] In the reaction kinetic model of the PCDD/F formations, the rate constant for the elementary reaction of

Table 1. Arrhenius Formulas (Units Are s^{-1} and cm^3 molecule^{-1} s^{-1} for Unimolecular and Bimolecular Reactions, Respectively) for the Elementary Reactions Involved in the Thermodynamically Favorable Formation Pathways of PBDDs from 2-BP, 2,4-DBP, and 2,4,6-TBP as Precursors over the Temperature Range of 600−1200 K
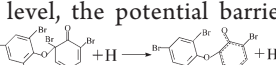
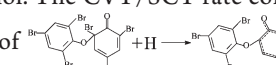| reactions	Arrhenius formulas
2-BP+H→2-BPR+H$_2$	$k(T)=(3.38 \times 10^{-11})\exp(-7384.78/T)$
2-BP+OH→2-BPR+H$_2$O	$k(T)=(5.34 \times 10^{-12})\exp(-2758.55/T)$
2-BP+O(^{3}P)→2-BPR+OH	$k(T)=(1.66 \times 10^{-11})\exp(-6404.68/T)$
2-BP+Cl→2-BPR+HCl	$k(T)=(1.71 \times 10^{-10})\exp(-1237.87/T)$
2-BP+Br→2-BPR+HBr	$k(T)=(1.93 \times 10^{-11})\exp(-3910.39/T)$
IM1+H→IM3+HBr	$k(T)=(5.85 \times 10^{-10})\exp(-3577.55/T)$
IM1+OH→IM3+HOBr	$k(T)=(2.07 \times 10^{-11})\exp(-3171.08/T)$
IM3→DD+Br	$k(T)=(5.67 \times 10^{11})\exp(-13390.79/T)$
IM2+H→IM5+H$_2$	$k(T)=(1.79 \times 10^{-11})\exp(-2692.33/T)$
IM5→1-MBDD+Br	$k(T)=(7.09 \times 10^{11})\exp(-13832.79/T)$
IM5→IM7	$k(T)=(2.55 \times 10^{12})\exp(-11951.40/T)$
IM7→IM10	$k(T)=(2.33 \times 10^{13})\exp(-7701.85/T)$
IM10→1-MBDD+Br	$k(T)=(7.40 \times 10^{11})\exp(-13268.05/T)$
2,4-DBP+H→2,4-DBPR+H$_2$	$k(T)=(6.83 \times 10^{-11})\exp(-7292.71/T)$
2,4-DBP+OH→2,4-DBPR+H$_2$O	$k(T)=(6.68 \times 10^{-12})\exp(-2690.13/T)$
2,4-DBP+O(^{3}P)→2,4-DBPR+OH	$k(T)=(4.71 \times 10^{-11})\exp(-5455.78/T)$
2,4-DBP+Cl→2,4-DBPR+HCl	$k(T)=(8.98 \times 10^{-11})\exp(-1231.28/T)$
2,4-DBP+Br→2,4-DBPR+HBr	$k(T)=(2.61 \times 10^{-10})\exp(-3518.55/T)$
IM11+H→IM13+HBr	$k(T)=(6.65 \times 10^{-11})\exp(-1967.34/T)$
IM11+OH→IM13+HOBr	$k(T)=(4.78 \times 10^{-12})\exp(-3419.21/T)$
IM13→2,7-DBDD+Br	$k(T)=(3.44 \times 10^{11})\exp(-14304.24/T)$
IM13→IM15	$k(T)=(1.41 \times 10^{12})\exp(-11816.21/T)$
IM15→IM18	$k(T)=(1.22 \times 10^{13})\exp(-7919.38/T)$
IM18→2,8-DBDD+Br	$k(T)=(4.41 \times 10^{11})\exp(-13097.41/T)$
IM12+H→IM19+H$_2$	$k(T)=(7.30 \times 10^{-13})\exp(-1141.98/T)$
IM19→1,3,8-TBDD+Br	$k(T)=(4.77 \times 10^{10})\exp(-14274.45/T)$
IM19→IM21	$k(T)=(1.90 \times 10^{12})\exp(-12032.47/T)$
IM21→IM24	$k(T)=(1.66 \times 10^{12})\exp(-7633.92/T)$
IM24→1,3,7-TBDD+Br	$k(T)=(2.40 \times 10^{11})\exp(-12767.14/T)$
2,4,6-TBP+H→2,4,6-TBPR+H$_2$	$k(T)=(4.15 \times 10^{-12})\exp(-7112.44/T)$
2,4,6-TBP+OH→2,4,6-TBPR+H$_2$O	$k(T)=(8.93 \times 10^{-12})\exp(-2368.10/T)$
2,4,6-TBP+O(^{3}P)→2,4,6-TBPR+OH	$k(T)=(6.30 \times 10^{-12})\exp(-5373.21/T)$
2,4,6-TBP+Cl→2,4,6-TBPR+HCl	$k(T)=(1.32 \times 10^{-10})\exp(-1032.16/T)$
2,4,6-TBP+Br→2,4,6-TBPR+HBr	$k(T)=(6.39 \times 10^{-10})\exp(-5381.05/T)$
IM25+H→IM26+HBr	$k(T)=(8.22 \times 10^{-11})\exp(-2370.52/T)$
IM25+OH→IM26+HOBr	$k(T)=(3.39 \times 10^{-12})\exp(-2564.09/T)$
IM26→1,3,6,8-TeBDD+Br	$k(T)=(1.06 \times 10^{12})\exp(-14774.34/T)$
IM26→IM27	$k(T)=(5.30 \times 10^{12})\exp(-11692.33/T)$
IM27→IM28	$k(T)=(1.95 \times 10^{13})\exp(-8337.48/T)$
IM28→1,3,7,9-TeBDD+Br	$k(T)=(6.91 \times 10^{11})\exp(-15447.33/T)$

Table 2. Arrhenius Formulas (Units Are s^{-1} and cm^3 molecule^{-1} s^{-1} for Unimolecular and Bimolecular Reactions, Respectively) for the Elementary Reactions Involved in the Formation of PBDFs from 2-BP, 2,4-BDP, and 2,4,6-TBP as Precursors over the Temperature Range of 600−1200 K

reactions	Arrhenius formulas
IM29+H→IM30+H$_2$	$k(T)=(9.75 \times 10^{-11})\exp(-1923.18/T)$
IM30→IM31	$k(T)=(3.77 \times 10^{12})\exp(-10251.93/T)$
IM31→IM32	$k(T)=(1.11 \times 10^{12})\exp(-11614.16/T)$
IM32→4,6-DBDF+OH	$k(T)=(3.10 \times 10^{13})\exp(-10683.59/T)$
IM29→IM33	$k(T)=(1.98 \times 10^{12})\exp(-9558.46/T)$
IM33+H→IM31+H$_2$	$k(T)=(2.44 \times 10^{-11})\exp(-5097.33/T)$
IM34+H→IM35+HBr	$k(T)=(2.17 \times 10^{-11})\exp(-2927.17/T)$
IM34+OH→IM35+HOBr	$k(T)=(1.63 \times 10^{-12})\exp(-2968.01/T)$
IM35→IM36	$k(T)=(1.39 \times 10^{12})\exp(-8079.76/T)$
IM36→IM37	$k(T)=(8.55 \times 10^{12})\exp(-16679.13/T)$
IM37→4-MBDF+OH	$k(T)=(2.77 \times 10^{13})\exp(-9572.70/T)$
IM38+H→IM39+H$_2$	$k(T)=(4.87 \times 10^{-11})\exp(-3260.61/T)$
IM39→IM40	$k(T)=(2.26 \times 10^{12})\exp(-8890.25/T)$
IM40→IM41	$k(T)=(1.75 \times 10^{12})\exp(-13935.26/T)$
IM41→2,4,6,8-TeBDF+OH	$k(T)=(1.89 \times 10^{13})\exp(-10713.53/T)$
IM38→IM42	$k(T)=(1.43 \times 10^{12})\exp(-9947.05/T)$
IM42+H→IM40+H$_2$	$k(T)=(2.17 \times 10^{-12})\exp(-5819.31/T)$
IM43+H→IM44+HBr	$k(T)=(3.65 \times 10^{-11})\exp(-1536.89/T)$
IM43+OH→IM44+HOBr	$k(T)=(2.61 \times 10^{-12})\exp(-2651.62/T)$
IM44→IM45	$k(T)=(2.04 \times 10^{12})\exp(-8320.15/T)$
IM45→IM46	$k(T)=(5.39 \times 10^{12})\exp(-16047.96/T)$
IM46→2,4,8-TBDF+OH	$k(T)=(2.87 \times 10^{13})\exp(-10379.37/T)$

are given in Table 1 for the elementary reactions involved in the thermodynamically favorable PBDD formation pathways and in Table 2 for the elementary reactions involved in the formation of PBDFs.

ASSOCIATED CONTENT

Ⓢ Supporting Information. Potential barriers ΔE (in kcal/mol) and reaction heats ΔH (in kcal/mol) for the formation of 2-BPRs, 2,4-DBPRs, and 2,4,6-TBPRs from 2-BP, 2,4-DBP, and 2,4,6-TBP. The total energies (in a.u.), the zero-point energies (ZPE, in a.u.), and the imaginary frequencies (in cm^{-1}) for the transition states. The geometries in terms of Cartesian coordinate (in Angstrom) for the reactants, products, intermediates, and transition states. This material is available free of charge via the Internet at http://pubs.acs.org.

AUTHOR INFORMATION

Corresponding Author
*Fax: 86-531-8836 1990. E-mail: zqz@sdu.edu.cn.

ACKNOWLEDGMENT

 +H ⟶ +HCl was assigned to be the value for the reaction of CH$_3$Cl+H→CH$_3$+HCl.[44,45] At 1000 K, the CVT/SCT rate constant for the elementary reaction of +H ⟶ +HBr is 7.68×10^{-12} cm^3 molecule^{-1} s^{-1}, which is larger than the experimental value of 4.49×10^{-12} cm^3 molecule^{-1} s^{-1} for the reaction of CH$_3$Br+H→ CH$_3$+HBr.[46] At the MPWB1K/6-311+G(3df,2p)// MPWB1K/6-31+G(d,p) level, the potential barrier for the elementary reaction of +H ⟶ +HBr is 2.80 kcal/mol, whereas the value for the reaction of CH$_3$Br+H→ CH$_3$+HBr is 6.89 kcal/mol. The CVT/SCT rate constant for the elementary reaction of +H ⟶ +HBr appears to be reasonable. To be used more effectively, the CVT/SCT rate constants are fitted, and Arrhenius formulas

1923

dx.doi.org/10.1021/es103536t |*Environ. Sci. Technol.* 2011, 45, 1917–1925

■ REFERENCES

(1) Samara, F.; Gullett, B. K.; Harrison, R. O.; Chu, A.; Clark, G. C. Determination of relative assay response factors for toxic chlorinated and brominated dioxins/furans using an enzyme immunoassay (EIA) and a chemically-activated luciferase gene expression cell bioassay (CALUX). *Environ. Int.* **2009**, *35* (3), 588–593.

(2) Samara, F.; Wyrzykowska, B.; Tabor, D.; Touati, D.; Gullett, B. K. Toxicity comparison of chlorinated and brominated dibenzo-*p*-dioxins and dibenzofurans in industrial source samples by HRGC/HRMS and enzyme immunoassay. *Environ. Int.* **2010**, *36* (3), 247–253.

(3) Mennear, J. H.; Lee, C. C. Polybrominated dibenzo-*p*-dioxins and dibenzofurans: literature review and health assessment. *Environ. Health Perspect.* **1994**, *102* (1), 265–274.

(4) Birnbaum, L. S.; Staskal, D. F.; Diliberto, J. J. Health effects of polybrominated dibenzo-*p*-dioxins (PBDDs) and dibenzofurans (PBDFs). *Environ. Int.* **2003**, *29* (6), 855–860.

(5) Olsman, H.; Engwall, M.; Kammann, U.; Klempt, M.; Otte, J.; van Bavel, B.; Hollert, H. Relative differences in aryl hydrocarbon receptor-mediated response for 18 polybrominated and mixed halogenated dibenzo-*p*-dioxins and -furans in cell lines from different species. *Environ. Toxicol. Chem.* **2007**, *26* (11), 2448–2454.

(6) Li, H. R; Feng, J. L; Sheng, G. Y.; Lü, S. L.; Fu, J. M.; Peng, P. A.; Man, R. The PCDD/F and PBDD/F pollution in the ambient atmosphere of Shanghai, China. *Chemosphere* **2008**, *70* (4), 576–583.

(7) Wang, L. C.; Tsai, C. H.; Chang-Chien, G. P.; Hung, C. H. Characterization of polybrominated dibenzo-*p*-dioxins and dibenzofurans in different atmospheric environments. *Environ. Sci. Technol.* **2008**, *42* (1), 75–80.

(8) Evans, C. S.; Dellinger, B. Formation of bromochlorodibenzo-*p*-dioxins and dibenzofurans from the high-temperature oxidation of a mixture of 2-chlorophenol and 2-bromophenol. *Environ. Sci. Technol.* **2006**, *40* (9), 3036–3042.

(9) Haglund, P. On the identity and formation routes of environmentally abundant tri- and tetrabromodibenzo-*p*-dioxins. *Chemosphere* **2010**, *78* (6), 724–730.

(10) Wang, L. C.; Wang, Y. F.; His, H. C.; Chang-Chien, G. P. Characterizing the emissions of polybrominated diphenyl ethers (PBDEs) and polybrominated dibenzo-*p*-dioxins and dibenzofurans (PBDD/Fs) from metallurgical processes. *Environ. Sci. Technol.* **2010**, *44* (4), 1240–1246.

(11) Ma, J.; Addink, R.; Yun, S.; Cheng, J. P.; Wang, W. H.; Kannan, K. Polybrominated dibenzo-*p*-dioxins/dibenzofurans and polybrominated diphenyl ethers in soil, vegetation, workshop-floor dust, and electronic shredder residue facility and in soils from a chemical industrial complex in eastern China. *Environ. Sci. Technol.* **2009**, *43* (19), 7350–7356.

(12) Wang, L. C.; His, H. C.; Wang, Y. F.; Lin, S. L.; Chang-Chien, G. P. Distribution of polybrominated diphenyl ethers (PBDEs) and polybrominated dibenzo-*p*-dioxins and dibenzofurans (PBDD/Fs) in municipal solid waste incinerators. *Environ. Pollut.* **2010**, *158* (5), 1595–1602.

(13) Wang, L. C.; Chang-Chien, G. P. Characterizing the emissions of polybrominated dibenzo-*p*-dioxins and dibenzofurans from municipal and industrial waste incinerators. *Environ. Sci. Technol.* **2007**, *41* (4), 1159–1165.

(14) Lai, Y. C.; Lee, W. J.; Li, H. W. Inhibition of polybrominated dibenzo-*p*-dioxin and dibenzofuran formation from the pyrolysis of printed circuit boards. *Environ. Sci. Technol.* **2007**, *41* (3), 957–962.

(15) Li, H. R.; Yu, L. P.; Sheng, G. P.; Fu, J. M.; Peng, P. A. Severe PCDD/F and PBDD/F pollution in air around an electronic waste dismantling area in China. *Environ. Sci. Technol.* **2007**, *41* (16), 5641–5646.

(16) Karasek, F. W.; Dickson, L. C. Model studies of polychlorinated dibenzo-*p*-dioxin formation during municipal refuse incineration. *Science* **1987**, *237* (4816), 754–756.

(17) Milligan, M. S.; Altwicker, E. R. Chlorophenol reactions on fly ash. 1. adsorption/desorption equilibria and conversion to polychlorinated dibenzo-*p*-dioxins. *Environ. Sci. Technol.* **1995**, *30* (1), 225–229.

(18) Evans, C.; Dellinger, B. Surface-mediated formation of polybrominated dibenzo-*p*-dioxins and dibenzofurans from the high-temperature pyrolysis of 2-bromophenol on a CuO/silica surface. *Environ. Sci. Technol.* **2005**, *39* (13), 4857–4863.

(19) Evans, C.; Dellinger, B. Formation of bromochlorodibenzo-*p*-dioxins and furans from the high-temperature pyrolysis of a 2-chlorophenol/2-bromophenol mixture. *Environ. Sci. Technol.* **2005**, *39* (20), 7940–7948.

(20) IUCLID, 2,4,6-tribromophenol and other simple brominated phenols, Data Set for 2,4,6-tribromophenol. Ispra, European Chemicals Bureau, International Uniform Chemical Information Database, 2003.

(21) Sim, W. J.; Lee, S. H.; Lee, I. S.; Choi, S. D.; Oh, J. E. Distribution and formation of chlophenols and bromophenols in marine and riverine environments. *Chemosphere* **2009**, *77* (4), 552–558.

(22) Na, Y. C.; Kim, K. J.; Park, C. S.; Hong, J. K. Formation of tetrahalogenated dibenzo-*p*-dioxins (TXDDs) by pyrolysis of a mixture of 2,4,6-trichlorophenol and 2,4,6-tribromophenol. *J. Anal. Appl. Pyrolysis* **2007**, *80* (1), 254–261.

(23) Sidhu, S. S.; Maqsud, L.; Dellinger, B. The homogeneous, gas-phase formation of chlorinated and brominated dibenzo-*p*-dioxin from 2,4,6-trichloro- and 2,4,6-tribromophenols. *Combust. Flame* **1995**, *100* (1–2), 11–20.

(24) Frisch, M. J.; Trucks, G. W.; Schlegel, H. B.; Gill, P. W. M.; Johnson, B. G.; Robb, M. A.; Cheeseman, J. R.; Keith, T. A.; Petersson, G. A.; Montgomery, J. A.; et al. GAUSSIAN 03, Pittsburgh, PA, 2003.

(25) Zhao, Y.; Truhlar, D. G. Hybrid meta density functional theory methods for therochemistry, thermochemical kinetics, and noncovalent interactions: The MPW1B95 and MPWB1K models and comparative assessments for hydrogen bonding and van der waals interactions. *J. Phys. Chem. A* **2004**, *108* (33), 6908–6918.

(26) Steckler, R.; Chuang, Y. Y.; Fast, P. L.; Corchade, J. C.; Coitino, E. L.; Hu, W. P.; Lynch, G. C.; Nguyen, K.; Jackells, C. F.; Gu, M. Z.; Rossi, I.; Clayton, S.; Melissas, V.; Garrett, B. C.; Isaacson, A. D.; Truhlar, D. G. POLYRATE Version 9.3; University of Minnesota: Minneapolis, 2002.

(27) Baldridge, M. S.; Gordor, R.; Steckler, R.; Truhlar, D. G. Ab initio reaction paths and direct dynamics calculations. *J. Phys. Chem.* **1989**, *93* (13), 5107–5119.

(28) Gonzalez-Lafont, A.; Truong, T. N.; Truhlar, D. G. Interpolated variational transition-state theory: Practical methods for estimating variational transition-state properties and tunneling contributions to chemical reaction rates from electronic structure calculations. *J. Chem. Phys.* **1991**, *95* (12), 8875–8894.

(29) Garrett, B. C.; Truhlar, D. G. Generalized transition state theory. Classical mechanical theory and applications to collinear reactions of hydrogen molecules. *J. Phys. Chem.* **1979**, *83* (8), 1052–1079.

(30) Fernandez-Ramos, A.; Ellingson, B. A.; Garret, B. C.; Truhlar, D. G. Variational Transition State Theory with Multidimensional Tunneling. In *Reviews in Computational Chemistry*; Lipkowitz, K. B., Cundari, T. R., Eds; Wiley-VCH: Hoboken, NJ, 2007.

(31) Senma, M.; Taira, Z.; Taga, T.; Osaki, K. Dibenzo-*p*-dioxin, $C_{12}H_8O_2$. *Crystallogr. Struct. Commun.* **1973**, *2* (2), 311–314.

(32) Landolt-Bornstein: Group II: Atomic and Molecular Physics Vol. 7: Structure Data of Free Polyatomic Molecules. Hellwege, K. H., Hellwege, A. M., Ed.; Springer-Verlag: Berlin, 1976.

(33) Ribeiro da Silva, M. A. V.; Lobo Ferreira, A. I. M. C. Gas phase enthalpies of formation of monobromophenols. *J. Chem. Thermodyn.* **2009**, *41* (10), 1104–1110.

(34) Lukyanova, V. A.; Kolesov, V. P.; Avramenko, N. V.; Vorobieva, V. P.; Golovkov, V. F. Standard enthalpy of formation of dibenzo-*p*-dioxin. *Zh. Fiz. Khim.* **1997**, *71* (3), 406–408.

(35) Chase, M. W., Jr. NIST-JANAF Themochemical Tables, 4th ed.; *J. Phys. Chem. Ref. Data*, Monograph 9, **1998**; 1-1951.

(36) Evans, C. S.; Dellinger, B. Mechanisms of dioxin formation from the high-temperature pyrolysis of 2-bromophenol. *Environ. Sci. Technol.* **2003**, *37* (24), 5574–5580.

(37) Evans, C. S.; Dellinger, B. Mechanisms of dioxin formation from the high-temperature oxidation of 2-bromophenol. *Environ. Sci. Technol.* **2005**, *39* (7), 2128–2134.

(38) Zhang, Q. Z.; Li, S. Q.; Qu, X. H.; Wang, W. X. A quantum mechanical study on the formation of PCDD/Fs from 2-chlorophenol as precursor. *Environ. Sci. Technol.* **2008**, *42* (19), 7301–7308.

(39) Na, Y. C.; Hong, J. K.; Kim, K. J. Formation of polybrominated dibenzo-*p*-dioxins/furans (PBDDs/Fs) by the pyrolysis of 2,4-dibromophenol, 2,6-dibromophenol, and 2,4,6-tribromophenol. *Bull. Korean Chem. Soc.* **2007**, *28* (4), 547–552.

(40) Zhang, Q. Z.; Yu, W. N.; Zhang, R. X.; Zhou, Q.; Gao, R.; Wang, W. X. Quantum chemical and kinetic study on dioxin formation from the 2,4,6-TCP and 2,4-DCP precursors. *Environ. Sci. Technol.* **2010**, *44* (9), 3395–3403.

(41) Weber, R.; Hagenmaier, H. Mechanism of the formation of polychlorinated dibenzo-*p*-dioxins and dibenzofurans from chlorophenols in gas phase reactions. *Chemosphere* **1999**, *38* (3), 529–549.

(42) Zhang, Q. Z.; Qu, X. H.; Xu, F.; Shi, X. Y.; Wang, W. X. Mechanism and thermal rate constants for the complete series reactions of chlorophenols with H. *Environ. Sci. Technol.* **2009**, *43* (11), 4105–4112.

(43) Xu, F.; Wang, H.; Zhang, Q. Z.; Zhang, R. X.; Qu, X. H.; Wang, W. X. Kinetic properties for the complete series reactions of chlorophenols with OH radicals—relevance for dioxin formation. *Environ. Sci. Technol.* **2010**, *44* (4), 1399–1404.

(44) Khachatryan, L.; Asatryan, R.; Dellinger, B. Development of expanded and core kinetic models for the gas phase formation of dioxins from chlorinated phenols. *Chemosphere* **2003**, *52* (4), 695–708.

(45) Khachatryan, L.; Burcat, A.; Dellinger, B. An elementary reaction-kinetic model for the gas-phase formation of 1,3,6,8- and 1,3,7,9-tetrachlorinated dibenzo-*p*-dioxins from 2,4,6-trichlorophenol. *Combust. Flame* **2003**, *132* (3), 406–421.

(46) Baulch, D. L.; Duxbury, J.; Grant, S. J.; Montague, D. C. Evaluated kinetic data for high temperature reactions. Volume 4 Homogeneous gas phase reactions of halogen- and cyanide- containing species. *J. Phys. Chem. Ref. Data* **1981**, *10* (Supplement 1), 1–721.